Dear Author,

Please, note that changes made to the HTML content will be added to the article before publication, but are not reflected in this PDF.

Note also that this file should not be used for submitting corrections.

Applied Clay Science xxx (2015) xxx–xxx

Contents lists available at ScienceDirect

Applied Clay Science

journal homepage: www.elsevier.com/locate/clay

Research paper

Preparation and antibacterial activity of chitosan-based nanocomposites containing bentonite-supported silver and zinc oxide nanoparticles for water disinfection

Sarah C. Motshekga [a,b], Suprakas Sinha Ray [a,c,*], Maurice S. Onyango [b], Maggie N.B. Momba [d]

[a] DST/CSIR National Centre for Nanostructured Materials, Council for Scientific and Industrial Research, Pretoria 0001, South Africa
[b] Department of Chemical, Metallurgical and Materials Engineering, Tshwane University of Technology, Pretoria 0001, South Africa
[c] Department of Applied Chemistry, University of Johannesburg, Doornfontein 2028, Johannesburg, South Africa
[d] Department of Environmental, Water and Earth Sciences, Tshwane University of Technology, Pretoria 0001, South Africa

ARTICLE INFO

Article history:
Received 12 January 2015
Received in revised form 2 June 2015
Accepted 6 June 2015
Available online xxxx

Keywords:
Bentonite chitosan nanocomposites
Gram-negative bacteria
Gram-positive bacteria
Antibacterial activity
Silver and zinc oxide nanoparticles

ABSTRACT

This study was conducted to develop novel chitosan nanocomposites and to optimize the minimum amount and contact time required to achieve complete inactivation of bacteria in water. Gram-negative *Escherichia coli* and Gram-positive *Enterococcus faecalis* bacteria were used to test the antibacterial activity of chitosan cross-linked with glutaraldehyde and chitosan nanocomposites in water. The silver and zinc oxide nanoparticles supported on bentonite were synthesized using microwave-assisted synthesis method. The resulting bentonite-supported silver and zinc oxide nanoparticles were dispersed in a chitosan biopolymer to prepare bentonite chitosan nanocomposites. The obtained bentonite chitosan nanocomposites were characterized with BET surface area measurements, FTIR, XRD, ICP-AES and SEM. When using cross-linked chitosan, it was demonstrated that factors such as pH, particle size and surface area influenced the inactivation of bacteria. For instance, the antibacterial activity of cross-linked chitosan was illustrated to increase with an increase in contact time. Meanwhile, an improvement in the inactivation activity was indicated with the introduction of silver and zinc oxide nanoparticles containing bentonite into the chitosan matrix. Although both silver and zinc oxide containing bentonite chitosan nanocomposites exhibited good antibacterial activity against bacteria, with removal efficiencies of at least 51%, the best antibacterial activity was demonstrated for silver–zinc oxide bentonite chitosan nanocomposite, with a removal efficiency of at least 78%. Furthermore, the antibacterial activity of bentonite chitosan nanocomposites was identified to be influenced by the amount of material, contact time and bacterial concentration. Finally, leaching tests demonstrated that bentonite chitosan nanocomposites were stable and, consequently, could be effectively used as antibacterial materials for water disinfection.

1. Introduction

The World Health Organization (WHO) estimates that more than 3.4 million people, many of them children, die each year from water related diseases. Globally, waterborne diseases are the second leading cause of death in children below the age of five years. It is estimated that 10% of diseases worldwide can be prevented by improving the water supply, sanitation, hygiene and management of water resources (Prüss-Üstün et al., 2008; WHO, 2013). The gravity of water shortages, including quality issues and their effects on the health of consumers, makes it necessary to direct considerable and focused efforts toward research and development programs in the drinking water sector (Savage and Diallo, 2005). WHO defines safe drinking water as water whose microbial, physical and chemical characteristics comply with their standards and national standards (WHO, 2006b). The greatest threat posed to drinking water resources arises from bacterial contamination. In addition to affecting the quality of water, bacterial contamination of water is a concern as they cause diseases that could be life-threatening upon ingestion or exposure. WHO recommends that any water intended for drinking purposes should contain fecal and total coliform counts of 0 in a 100 ml sample (WHO, 2006a). Given these concerns, many traditional treatment methods, both chemical (chlorine, ozone, iodine) and physical (ultraviolet light, radiation) (Boorman et al., 1999; Woo et al., 2002; Tiwari et al., 2008), have been applied to inactivate bacteria in water supplies. Although these methods can effectively reduce and control pathogenic bacteria to the desired levels, in recent years, research has revealed that such methods can lead to the formation of harmful disinfection byproducts (DBP) (Richardson, 2003a; Krasner et al., 2006).

Chemical disinfectants such as chlorine and ozone can react with various constituents of water to form DBP that are carcinogenic. However, one of the most complex and important challenges in water treatment

* Corresponding author. Fax: +27 12 841 2229.
E-mail address: rsuprakas@csir.co.za (S.S. Ray).

http://dx.doi.org/10.1016/j.clay.2015.06.010
0169-1317/

is that some of these bacteria have become increasingly resistant to the available disinfectants and now require extremely high disinfectant doses, leading to the formation of greater abundance of DBP. Therefore, there is an urgent need to re-evaluate conventional disinfection methods and to consider innovative approaches that can offer enhanced reliability and robustness of disinfection while avoiding DBP formation (Richardson, 2003b, 2004; Li et al., 2008). Apart from DBP formation, the above technologies are often costly and time-consuming.

In the past two decades, advances in nanoscience and nanotechnology have expanded the possibilities for the development of high-performance nanomaterials targeted at solving the current problems related to water quality. There are four classes of nanoscale materials that are being evaluated for use as functional materials for water treatment: (1) metal/oxide nanoparticles, (2) carbonaceous nanomaterials, (3) zeolites and (4) dendrimers. These materials possess a broad range of physico-chemical properties that make them attractive for use as separation and reactive media for water treatment (Savage and Diallo, 2005; Tiwari et al., 2008). They can also be functionalized with various chemical groups to increase their affinity toward a given compound. They can be prepared as nanosorbents, nanocatalysts and reactive membranes and, therefore, exhibit promising and enhanced properties of selective bacteria inactivation and removal (Savage and Diallo, 2005; Tiwari et al., 2008; Ray et al., 2012). Moreover, given the concerns regarding the treatment resistance of pathogenic bacteria in water, the search for new disinfection agents has become a critical issue.

Silver (Ag) nanoparticles have drawn considerable interest for water disinfection because of their antibacterial activity, and they have attracted application in various consumer products (Lin et al., 2012). Ag nanoparticles are a well-known disinfectant that is effective for a wide spectrum of bacteria and viruses. It is thought to be more effective and is more widely used for Gram-negative bacteria. Drinking water often contains a broad range of both types of bacteria (Gram-negative and Gram-positive). Therefore, the treatment of water in which both types are likely to be present with a disinfectant that has been reported to be more effective against Gram-negative bacteria makes it difficult to achieve complete inactivation of bacteria (Shahverdi et al., 2007; Theivasanthi and Algar, 2011; dos Santos et al., 2012). Consequently, this approach will compromise the effectiveness of the disinfectant and increase the amount required. To compensate for this shortcoming and achieve thorough inactivation for a wide spectrum of bacteria, inorganic metal/oxide nanoparticles are often combined to form nanoparticle hybrids. Among the inorganic metal oxide nanoparticles that have been tested extensively for their antibacterial activity are zinc oxide (ZnO) nanoparticles. ZnO nanoparticles have been studied extensively using various pathogenic and non-pathogenic bacteria. They have also been reported to possess strong antibacterial activity against a broad range of bacteria (Reddy et al., 2007; Jones et al., 2008; Li et al., 2008; Azam et al., 2012; Motshekga et al., 2013). Therefore, it is highly probable that a combination of Ag and ZnO nanoparticles will be effective against both Gram-negative and Gram-positive bacteria that are typically found in water. Both Ag and ZnO nanoparticles possess larger surface areas for interaction and higher reactivity than the corresponding bulk materials and therefore produce stronger antibacterial effects (Emami-Karvani and Chehrazi, 2011; Azam et al., 2012). These unique properties make nanoparticles appealing compared to their bulk counterparts. However, the disadvantage of nanoparticles is that when used as individual components of functional materials, they tend to agglomerate, which reduces their effectiveness. Another disadvantage is that the release of nanoparticles into the environment during the treatment process poses a health risk, as the toxicity effect to the end user is not well known. For nanoparticles to be applied effectively for water disinfection, they typically must be supported on substrates such as carbon nanotubes, clays or polymers (Savage and Diallo, 2005; Li et al, 2008; Tiwari et al., 2008).

Clays and clay minerals are an excellent material for this purpose given the various relevant concerns. Clays such as bentonite and clay minerals such as montmorillonite, kaolinite, palygorskite and halloysites have been used as supporting substrates for nanoparticles in various water purification systems (Yavuza et al., 2003; Meteš et al., 2004; Bhattacharyya and Gupta, 2006; Karapinar and Donat, 2009). They can be used as individual components or as substrates for composite materials. Bentonite (Bent), which consists of more than 70% montmorillonite, has attracted considerable interest because it is easily available in bulk quantities, economically attractive and environmentally friendly and because it possess excellent swelling and adsorption properties. Bent has been used as a support to disperse and stabilize nanoparticles in various applications (Ayari et al., 2005; Hashemian, 2010; Zamparas et al., 2012).

Although there are numerous studies regarding the antibacterial activity of clay-supported metal/oxide nanoparticles, most have used the disk diffusion method to test their antibacterial effect, and no reports of further water treatment applications of these materials are available in the literature (Magaña et al., 2008; Santos et al., 2011; Shameli et al., 2011a; Hrenovic et al., 2012; Bagchi et al., 2013). To limit the leaching of nanoparticles into the water, clays that contain metal/oxide nanoparticles are often imbedded in various polymer matrices. Therefore, the robustness of applying these metal or metal oxide nanoparticles decorated clays in water disinfection is established when they are incorporated within a polymer. In this work, chitosan (Cts) biopolymer was used as a matrix. Cts is the second most plentiful natural biopolymer. It was chosen because it is non-toxic and possesses inherent antimicrobial properties. However, the antimicrobial activity of Cts is affected by a number of factors, including its molecular mass, the species and concentration of the bacteria, and the type and pH of the solution. Cts has also been widely used as an adsorbent for transition-metal ions and organic species because the amino (—NH_2) and hydroxyl (—OH) groups on Cts chains can serve as coordination and reaction sites (Zheng and Zhu, 2003; Chang and Juang, 2004; Li et al., 2008; Raafat and Sahl, 2009; Kittinaovarat et al., 2010; Guibal et al., 2013).

To date, few studies have been performed concerning the antibacterial activities of clay polymer nanocomposites, although such studies are necessary and significant. In this study, Bent was used as a supporting substrate for Ag, ZnO and Ag–ZnO nanoparticles. A facile microwave-assisted synthesis method was employed for the impregnation of the nanoparticles on the clay, while solvent-casting method was used to disperse nanoparticles containing clay in the Cts matrix. The obtained Bent Cts nanocomposites were therefore expected to demonstrate effective antibacterial activity against *Escherichia coli* (*E. coli*) and *Enterococcus faecalis* (*E. faecalis*) bacteria, which served as representatives of Gram-negative and Gram-positive bacteria, respectively.

2. Materials and methods

2.1. Materials

Pristine Bent, which was used as the solid support for Ag, ZnO and Ag–ZnO nanoparticles, was obtained from Ecca Holdings (Pty) Ltd, South Africa. Cts was purchased from Sigma Aldrich (South Africa) as a flake material. Glutaraldehyde (GLA, 50 wt.% in H_2O); phosphate buffered saline (PBS, pH 7.4); sulfuric acid (H_2SO_4, 98%); acetic acid ($C_2H_4O_2$, 99%); sodium chloride (NaCl); sodium hydroxide pellets (NaOH); silver nitrate ($AgNO_3$, 99.98%), which was used as the Ag precursor; and ZnO nanoparticles dispersed in ethanol were purchased from Sigma Aldrich, South Africa. All aqueous solutions were prepared using distilled water. Sodium thiosulfate ($Na_2S_2O_3$), nutrient broth and nutrient agar were purchased from Merck, South Africa. The bacterial strains used to provide the antibacterial activity were Gram-negative *E. coli* (ATCC 11775) and Gram-positive *E. faecalis* (ATCC 14506) from the American Type Culture Collection.

Please cite this article as: Motshekga, S.C., et al., Preparation and antibacterial activity of chitosan-based nanocomposites containing bentonite-supported silver and zinc oxide nanoparticles for water disinfection, Appl. Clay Sci. (2015), http://dx.doi.org/10.1016/j.clay.2015.06.010

2.2. Cross-linking of Cts with GLA

Cross-linked Cts was prepared by dissolving 1 wt.% Cts flakes into a 1% (v/v) aqueous $C_2H_4O_2$ solution and stirring overnight at 50 °C and 500 rpm until a clear solution was obtained. The solution was centrifuged to remove insoluble Cts. The solution pH was then adjusted to 5. The Cts solution was added dropwise using a disposable syringe pump into 1 M NaOH under gentle stirring and stirred overnight to neutralize the acid. The resulting Cts beads were extensively rinsed and filtered with distilled water to remove any residual NaOH. The wet beads (now irregular in shape after filtering) were then dispersed in 1% GLA solution and stirred overnight. The cross-linked Cts beads were extensively washed to remove excess GLA solution. Finally, the beads were air dried at 30 °C for 4 h, followed by an increase in temperature to 70 °C overnight. The beads were then ground and sieved to a constant size of <400 μm before use.

2.3. Synthesis of Ag, ZnO and Ag–ZnO nanoparticles containing Bent

Metal and metal oxide containing Bent were synthesized as reported in a previous study (Motshekga et al., 2013), and used without any further modification. In brief, three different batches of Ag-containing Bent (Ag Bent), ZnO-containing Bent (ZnO Bent), and both Ag and ZnO-containing Bent (Ag–ZnO Bent) were prepared using microwave-assisted synthesis method. The Bent nanocomposites were characterized and stored for later use.

2.4. Synthesis of Bent Cts nanocomposites

The preparation method for Bent Cts nanocomposites (Ag Bent Cts nanocomposite, ZnO Bent Cts nanocomposite and Ag–ZnO Bent nanocomposite) was modified from previously reported procedures (Wang et al., 2005; Kamari et al., 2009). A Cts solution was prepared by dissolving 1 wt.% Cts flakes into a 1% (v/v) aqueous $C_2H_4O_2$ solution and stirring overnight at 50 °C and 500 rpm until a clear solution was obtained. The solution was centrifuged to remove insoluble Cts. The solution was then adjusted to pH 5. To obtain clay dispersion, 1.0 g of each Bent nanocomposite (such as Ag Bent, ZnO Bent and Ag–ZnO Bent) was first dispersed in 250 ml of distilled water, followed by stirring at 200 rpm for an hour at room temperature. The stirring was increased to 500 rpm, and 250 ml of Cts solution was slowly added to each Bent dispersion. The mixtures were left stirring overnight at room temperature. The Bent Cts dispersions were added dropwise using a disposable syringe pump into 1 M NaOH solution under gentle stirring and stirred overnight to neutralize the acid. The resulting Bent Cts nanocomposite beads were extensively rinsed and filtered with distilled water to remove any residual NaOH. The wet beads (now irregular in shape after filtering) were then dispersed in 1% GLA solution and stirred overnight. The cross-linked Bent Cts nanocomposite beads were extensively washed to remove excess GLA solution. Finally, the beads were air dried at 30 °C for 4 h, followed by an increase in temperature to 70 °C overnight. The beads were then ground and sieved to a constant size of <400 μm before use.

2.5. Preparation of synthetic bacteria-contaminated water

The bacterial activities of the prepared Bent Cts nanocomposites (Ag Bent Cts nanocomposite, ZnO Bent Cts nanocomposite and Ag–ZnO Bent Cts nanocomposite) were evaluated against *E. coli* (ATCC 11775) and *E. faecalis* (ATCC 14506) as model test strains for Gram-negative and Gram-positive bacteria, respectively. These bacterial strains were obtained from the American Type Culture Collection (Quantum Biotechnologies, RSA). The strains were confirmed through cultural tests using selective agar media in accordance with the Standard Methods (Standard Methods, 1998).

Bacterial strains were maintained on nutrient agar (Merck, South Africa) plates and incubated at 36 ± 1 °C for 24 h. One loop of each organism was grown in 100 ml of sterile nutrient broth (Merck, South Africa) in a 250 ml flask. The flasks were incubated overnight in a shaking incubator (Scientific Model 353, Lasec South Africa) at 120 rpm for 24 h. The bacteria were harvested via centrifugation at 3500 rpm for 15 min and washed twice with 50 ml of sterile 0.01 M PBS (pH 7.4). Stock solutions were prepared by redispersing the final pellets in 10 ml of PBS solution. For each test bacterium, 1 ml of an overnight culture was serially diluted into 9 ml of sterile physiological water (0.9% w/v NaCl) and spread plated onto selective agar plates. The plates were incubated at36 ± 1 °C for 24 h, and the resulting colonies were counted to determine the initial bacterial concentrations in units of cfu/ml. For each target bacterium, aliquots of the overnight cultures corresponding to approximately 5×10^2, 5×10^3 and 5×10^4 cfu/ml were inoculated into 2 l or 5 l glass bottles containing the final volumes of sterile normal saline water (0.9% w/v). The spiked water samples were prepared freshly each day and shaken vigorously several times prior to being used in testing against Bent Cts nanocomposites. All experiments were performed in triplicate.

2.6. Bactericidal experiments

Samples of each Bent Cts nanocomposite (Ag Bent Cts nanocomposite, ZnO Bent Cts nanocomposite and Ag–ZnO Bent nanocomposite) in amounts of 0.3, 0.4 and 0.5 g (to evaluate the minimum amount required for complete inactivation of bacteria) were weighed into Falcon test tubes. The tubes were filled with 20 ml of contaminated water and shaken at 36 ± 1 °C in a water-bath shaker (Jalubo SW22, Labotec South Africa) at 160 rpm for 60 min. To evaluate the influence of contact time between the contaminated water and Bent Cts nanocomposites on the inactivation of bacteria, aliquots were drawn after 2 min, 5 min, 10 min, 20 min, 30 min, 40 min, 50 min and 60 min. At each time interval, 100 μl was withdrawn from each tube into micro test tubes, which contained 1 ml of $Na_2S_2O_3$, to terminate the disinfection reaction. The aliquots were plated onto nutrient agar without any further dilution to count the bacterial colonies. Controls containing bacteria but no Bent Cts nanocomposites were also included in the experiment. The plates were incubated at 36 ± 1 °C for 24 h. After the incubation period, the colonies on each plate were counted using a colony counter. All antibacterial tests were performed in triplicate, and the averaged results are reported.

2.7. Leaching tests

To evaluate the stability of the nanoparticles in the Bent Cts nanocomposites, leaching tests were performed. A sample of 0.2 g of each Bent Cts nanocomposite (Ag Bent Cts nanocomposite, ZnO Bent Cts nanocomposite and Ag–ZnO Bent Cts nanocomposite) material was immersed in 20 ml of distilled water and vigorously shaken in a water-bath shaker (at 36 ± 1 °C, 200 rpm) for various time periods. After shaking, a fraction of each dispersion was drawn. The samples were analyzed using inductively coupled plasma atomic emission spectroscopy (ICP-AES, PerkinElmer, USA) to determine the quantity of the nanoparticles that had leached into the water.

2.8. Characterization

The surface morphology and dispersion of Bent in the Cts matrix were analyzed using a scanning electron microscopy (Zeiss Ariga SEM, Germany). The samples were mounted on a copper stub using carbon tape and sputter coated with carbon to avoid charging. Energy-dispersive X-ray spectroscopy (EDS) analysis of the Bent Cts nanocomposites was performed at various points to obtain a qualitative determination of the elemental composition of the Ag and ZnO (as Zn) nanoparticles. The crystalline phases of the samples were determined

Please cite this article as: Motshekga, S.C., et al., Preparation and antibacterial activity of chitosan-based nanocomposites containing bentonite-supported silver and zinc oxide nanoparticles for water disinfection, Appl. Clay Sci. (2015), http://dx.doi.org/10.1016/j.clay.2015.06.010

via powdered X-ray diffraction (XRD, PANalytical XPERT-PRO diffractometer, the Netherlands) measurements using Ni-filtered CuKα radiation (λ = 1.5406 Å) and a variable slit at 35 kV and 50 mA. BET (Brunauer, Emmett, and Teller) surface area and pore size measurements of Bent Cts nanocomposites were performed using a Micromeritics TRISTAR 3000 (USA) surface area analyzer via the low-temperature N_2 adsorption method. Prior to analysis, the samples were degassed at 50 °C overnight under a continuous flow of N_2 gas to remove volatile moisture and adsorbed contaminants from the surfaces and pores of the Bent Cts nanocomposites. Fourier transform infrared spectroscopy (FTIR) spectra were recorded using a PerkinElmer Spectrum100 (USA) spectrometer equipped with a germanium crystal.

3. Results and discussion

3.1. BET surface area and pore size

The BET surface area and pore size analyses of cross-linked Cts and Bent Cts nanocomposites are summarized in Table 1. The cross-linked Cts presented a low surface area of 0.0695 m^2/g and a pore size of 86 nm. From these results, it is apparent that the low surface area of Cts indicates that the physical adsorption of Bent (Ag Bent, ZnO Bent and Ag–ZnO Bent) onto the surface is not possible, whereas the large pore size allows for nanoparticles to be deposited within the pores of Cts, as was confirmed from the reduced pore sizes of Bent Cts nanocomposites (Table 1). With regard to antibacterial activity, these findings could also mean that adsorption/adhesion of bacterial cells on the Cts surfaces would not be possible. Such a characteristic would be advantageous because it would indicate that Bent Cts nanocomposites could be potential antibacterial disinfectants. A considerable increase in the BET surface area with respect to that of Cts was demonstrated for all Bent Cts nanocomposites: Ag Bent Cts nanocomposite, ZnO Bent Cts nanocomposite and Ag–ZnO Bent Cts nanocomposite. A large surface area implies better interaction between the Bent Cts nanocomposites and the bacteria. Similarly, a comparable decrease in the pore sizes of Bent Cts nanocomposites was demonstrated. These observations could be attributable to the deposition of the nanoparticles within the larger pores of Cts matrix. These results confirm the observation from SEM images (as discussed latter) that the morphology of Cts was modified by the addition of Ag Bent, ZnO Bent and Ag–ZnO Bent nanocomposites.

3.2. Powder XRD studies

Fig. 1 presents the XRD patterns of cross-linked Cts and Bent Cts nanocomposites (Ag Bent Cts nanocomposite, ZnO Bent Cts nanocomposite and Ag–ZnO Bent Cts nanocomposite). The presence of the two broad reflections at 2θ = 6.94° and 20° in the XRD results for Cts indicates poor crystallinity. A typical XRD pattern of Cts is characterized by two sharp reflections at 2θ = 10° and 20°. The results obtained in this study are in agreement with previous studies (Wang et al., 2005; Beppu et al., 2007; Li et al., 2013), in which the crystallinity of Cts was found to decrease after cross-linking with GLA. This phenomenon has been attributed to the deformation of the hydrogen bond in the Cts caused by the substitution of the —OH and —NH_2 groups, which destroys Cts chains and results in the formation of amorphous GLA cross-linked Cts (Li et al., 2013). The reflections that appeared at

Table 1
BET surface area and pore size measurements of cross-linked Cts, Ag Bent Cts nanocomposite, ZnO Bent Cts nanocomposite and Ag–ZnO Bent Cts nanocomposite.

Samples	BET surface area/m^2 g^{-1}	Pore size/nm
Cts	0.0695 ± 0.017	86.54 ± 0.23
Ag Bent Cts nanocomposite	3.4685 ± 0.008	15.67 ± 1.11
ZnO Bent Cts nanocomposite	2.9189 ± 0.27	20.90 ± 1.09
Ag–ZnO Bent Cts nanocomposite	3.1812 ± 0.2877	17.96 ± 0.11

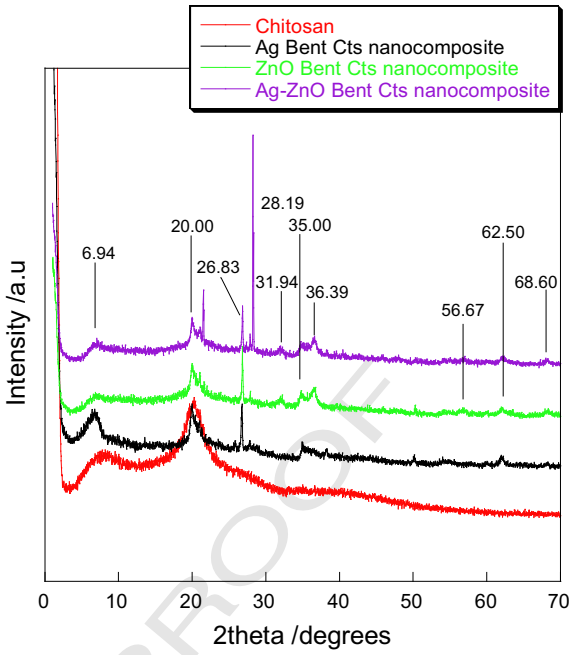

Fig. 1. XRD spectra of cross-linked Cts and Bent Cts nanocomposites.

2θ = 26° and 28°, are attributed to Bent as indicated in the Bent Cts nanocomposites and not identified in the XRD reflection of Cts. These findings are corroborated with the published literature (Wang et al., 2005; Motshekga et al., 2013). The XRD pattern of Bent Cts nanocomposites reveals that the characteristic reflections of Bent which appeared at 2θ = 6°, 20° and 35°, overlap with those of Cts. Although the first two reflections of Bent were not identified due to this overlap, the 35° reflection was identified in all Bent Cts nanocomposites. Slightly shifted reflection corresponding to Ag nanoparticle in Ag Bent Cts nanocomposites, attributed to the crystallographic planes of the face-centered cubic silver crystals, was identified at 35° and 62°, in agreement with previous studies (Shameli et al., 2011b; Quang and Chau, 2013). Other reflections at 2θ = 31.94°, 36.39°, 56.67°, 62.50° and 68.60° were assigned to the wurtzite structure of hexagonal ZnO (Li et al., 2010; Raghupathi et al., 2011; Talebian et al., 2013). In addition, Q8 the characteristic reflection at 2θ = 62°, which overlaps with reflections associated with Ag and ZnO, is assigned to Bent (Shameli et al., 2010). All reflections of Cts, Bent and Ag and ZnO nanoparticles were evident in the Bent Cts nanocomposite samples, reflecting the successful formation of clay polymer nanocomposite.

3.3. FTIR analysis

FTIR measurements were performed to identify possible interactions between Bent nanocomposites and the Cts matrix. Typical FTIR spectra of cross-linked Cts and Bent Cts nanocomposites are presented in Fig. 2. In the spectrum of cross-linked Cts, the strong broad band indicated at 3338 cm^{-1} can be assigned to the N—H stretching vibration of —NH_2 groups. The presence of the 2885 cm^{-1} band corresponds to the C—H stretching vibration of —CH_2 groups, the 1656 and 1559 cm^{-1} bands to N—H bending, the 1363 cm^{-1} band to C—H bending, and the intense band at 1033 cm^{-1} is assigned to C—O stretching (Beppu et al., 2007; Li et al, 2013). The Cts spectrum exhibits typical characteristics of Cts as reported in the literature, and all these bands are also present in the spectra of Bent Cts nanocomposites. The interlayered O—H group band at 3630 cm^{-1} originating from the clay in the Bent Cts nanocomposites was identified with a relatively low intensity. On the other hand, the bands of Si—O—Si, which are characteristic of phyllosilicate minerals, were revealed at 1006 cm^{-1} and 796 cm^{-1} in the absence of Cts (Motshekga et al., 2013). Upon the

Please cite this article as: Motshekga, S.C., et al., Preparation and antibacterial activity of chitosan-based nanocomposites containing bentonite-supported silver and zinc oxide nanoparticles for water disinfection, Appl. Clay Sci. (2015), http://dx.doi.org/10.1016/j.clay.2015.06.010

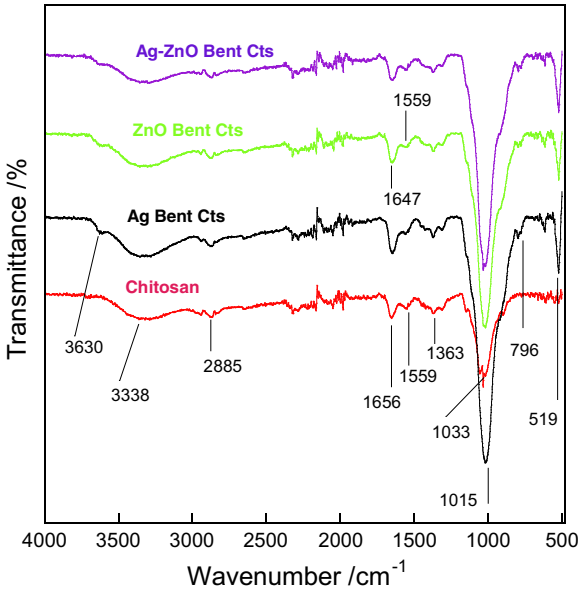

Fig. 2. FTIR spectra of cross-linked Cts and Bent Cts nanocomposites.

addition of Cts, the band at 1006 cm^{-1} shifted slightly to 1015 cm^{-1} and manifested as a very intense, sharp band, while the band at 796 cm^{-1} remained the same. The bands of —NH_2 group appeared at 1656 and 1559 cm^{-1}. The band at 1656 cm^{-1} shifted to 1647 cm^{-1} in the Bent Cts nanocomposites, while the band at 1559 cm^{-1} remained in the same position but exhibited a reduced intensity (Shameli et al., 2010). These results indicate an interaction between the clay and the Cts, with some bands overlapping each other. Another band was identified at 519 cm^{-1} in the Bent Cts nanocomposites samples; this band has been assigned to the bending vibration of Al—O—Si in octahedral sheets of the clay (Özcan and Özcan, 2004; Shameli et al., 2010; El-Sherif and El-Masry, 2011). These results also demonstrate that with the presence of Ag Bent, ZnO Bent and Ag–ZnO Bent in the Cts matrix, the bands shifted to lower wavenumbers (from 1656 to 1647 cm^{-1}), while the band intensities either increased or decreased (the band at 1015 cm^{-1} manifested as a sharp band in the Bent nanocomposites, compared to pristine Bent as reported in the literature and 1656 cm^{-1} band increased in intensity in the Bent Cts nanocomposites) indicating the interaction between the Bent and Cts in Bent Cts nanocomposites

3.4. Surface morphology and elemental analysis

SEM is a widely used technique for studying the morphology and cross-sectional surface characteristics of materials. In the present study, SEM was used to assess morphological changes in Bent nanocomposites encapsulated in cross-linked Cts. The cross-linked Cts [parts (a) and (b) of Fig. 3] exhibited a dense and uniform plain morphology, indicating that Cts was chemically modified by GLA. This observation is consistent with the results of previous studies in which GLA has

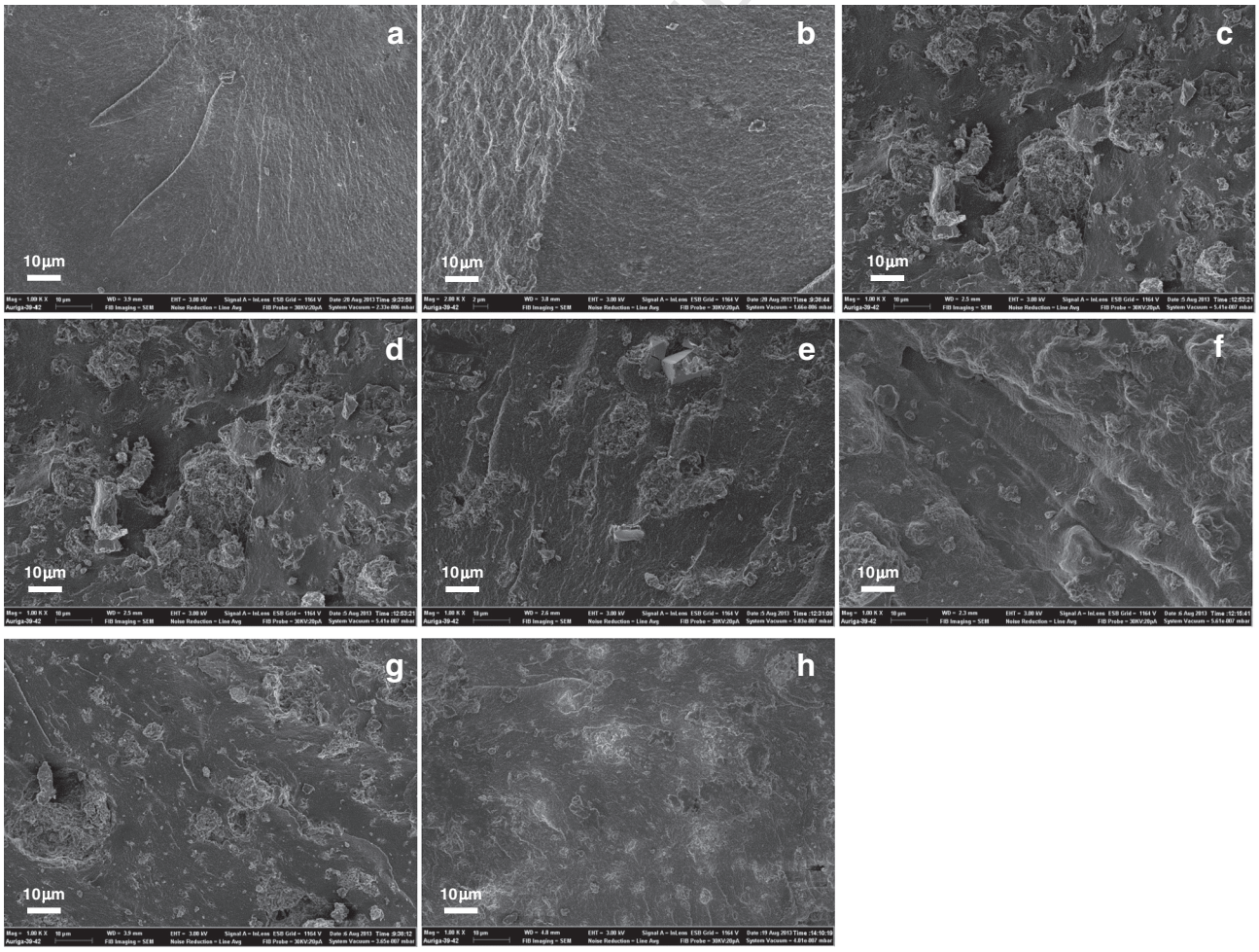

Fig. 3. SEM micrographs of cross-linked Cts and Bent Cts nanocomposites: (a–b) cross-linked Cts, (c–d) Ag Bent Cts nanocomposite; (e–f) ZnO Bent Cts nanocomposite and (g–h) Ag–ZnO Bent Cts nanocomposite.

Please cite this article as: Motshekga, S.C., et al., Preparation and antibacterial activity of chitosan-based nanocomposites containing bentonite-supported silver and zinc oxide nanoparticles for water disinfection, Appl. Clay Sci. (2015), http://dx.doi.org/10.1016/j.clay.2015.06.010

been used as a cross-linking agent (Anirudhan and Rijith, 2009; Li et al., 2013). Although the cross-linked Cts exhibited a relatively rough morphology, Bent Cts nanocomposites exhibited a significant rougher morphology, with numerous protruding bulk-like agglomerates, as illustrated in parts (c) to (d) of Fig. 3 (Ag Bent Cts nanocomposite), parts (e) to (f) of Fig. 3 (ZnO Bent Cts nanocomposite) and parts (g) to (h) of Fig. 3 (Ag–ZnO Bent Cts nanocomposite). The morphology of the Bent Cts nanocomposites clearly indicated the presence of Ag Bent, ZnO Bent and Ag–ZnO Bent. Aggregated particle structures were identified for all Bent Cts nanocomposites. The agglomeration of the particles may be attributable to poor mixing and the difference in the viscosities of the solutions, which may have caused the more viscous solution to encapsulate the less viscous one before proper mixing could be achieved. The elemental composition of Bent Cts nanocomposites was studied via EDS. Parts (a) to (c) of Fig. 4 depict the EDS analysis of selected areas. The EDS analysis confirmed that ZnO Bent Cts nanocomposite and Ag–ZnO Bent Cts nanocomposite contained approximately 18 wt.% and 21 wt.% ZnO, respectively, whereas the Ag Bent Cts nanocomposite and Ag–ZnO Bent Cts nanocomposite contained 3.9 wt.% and 1.7 wt.% Ag, respectively. The results indicate a large quantity of ZnO compared with Ag. However, it was not possible to measure the actual size of the impregnated Ag and ZnO nanoparticles in the Cts matrix, as was done for Ag Bent, ZnO Bent and Ag–ZnO Bent nanocomposites in a previous study (Motshekga et al., 2013). Thus, the sizes of Ag and ZnO nanoparticles in the Cts matrix were assumed to be 9–30 nm and 15–70 nm, respectively, as was determined using the TEM technique in the previous study. The sizes of nanoparticles have a considerable effect on their antibacterial activity, as they determine how easily nanoparticles are able to penetrate through bacterial walls. The presence of other elements (Al, C, Si, Fe, Mg, etc.), which originated from Cts and Bent, were also detected. The analysis also identified the presence of carbon, which originated from the carbon coating of Bent Cts nanocomposites prior to SEM analysis.

3.5. Leaching studies

The leaching rates of Ag and ZnO (as Zn) nanoparticles into the water were analyzed via ICP-AES, and the results are summarized in Tables 2 and 3. The release of nanoparticles from Bent Cts nanocomposites could affect the stability and application of these materials in drinking water disinfection, which is of great significance. Moreover, metal/oxide nanoparticles may cause adverse effects on consumers and the environment when their concentration is above the recommended levels. The accepted concentrations for Ag and Zn in drinking water as defined by WHO are 0.1 mg/l and 3–5 mg/l, respectively (WHO, 2011). Water above these levels is not allowed to be used for consumption. The ICP analyses performed in this study demonstrated that Ag nanoparticles were released into the water in small amounts of 0.01 mg/l after shaking for 30 min, which increased to 0.050 and 0.069 mg/l after contact times of 4 and 12 h, respectively. These findings confirm the stability of the nanoparticles within the Bent Cts nanocomposites under adverse shaking conditions. Regiel et al. (2013) have reported a strong attachment of Ag nanoparticles on Cts with a different molecular mass; therefore, the low leaching rates revealed in this study could be expected. Although the leaching of Zn was higher and more inconsistent, the leached amount was still below the allowable levels. Fluctuations in the leaching rate of Zn were indicated in all Bent Cts nanocomposites that contained ZnO, and the relative stability of Ag was also confirmed in all Bent Cts nanocomposites. The fluctuations in leaching may be attributed to the grinding process and the quantity of nanoparticles within the Bent Cts nanocomposites. During the grinding process to prepare samples of < 400 μm, the nanoparticles became partially exposed from the polymer; some were left loose and were therefore able to leach into the water immediately upon coming in contact with the water. To confirm this hypothesis, an ICP analysis of Bent Cts nanocomposites before the grinding process was performed

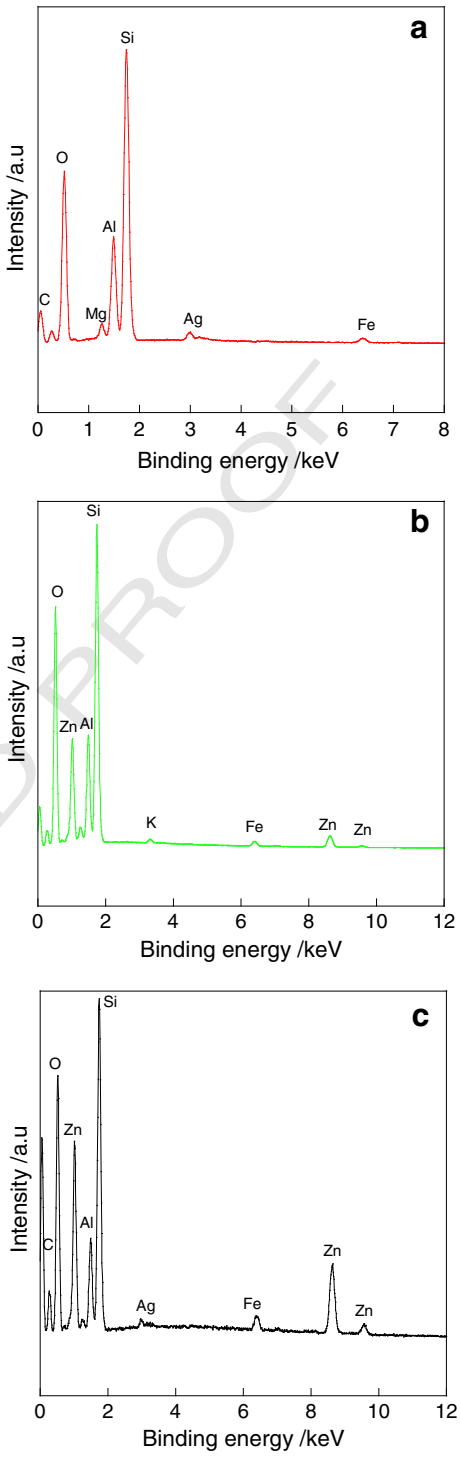

Fig. 4. EDS analysis of (a) Ag Bent Cts nanocomposite, (b) ZnO Bent Cts nanocomposite and (c) Ag–ZnO Bent Cts nanocomposite.

Table 2
Leaching-test analysis of Ag and ZnO nanoparticles from Bent Cts nanocomposites.

Samples		0 min	30 min	60 min	4 h	12 h
Ag Bent Cts nanocomposite	Ag	<0.005	0.010	0.023	0.050	0.069
ZnO Bent Cts nanocomposite	Zn	<0.020	0.270	0.160	0.180	0.220
Ag–ZnO Bent Cts nanocomposite	Ag	<0.005	0.008	0.011	0.023	0.022
	Zn	<0.020	<0.02	0.047	0.440	0.460

Please cite this article as: Motshekga, S.C., et al., Preparation and antibacterial activity of chitosan-based nanocomposites containing bentonite-supported silver and zinc oxide nanoparticles for water disinfection, Appl. Clay Sci. (2015), http://dx.doi.org/10.1016/j.clay.2015.06.010

Table 3
Leaching-test analysis of Ag and ZnO nanoparticles from Bent Cts nanocomposites (before grinding).

Samples		30 min	4 h
Ag Bent Cts nanocomposite	Ag	<0.005	0.010
ZnO Bent Cts nanocomposite	Zn	<0.020	<0.020
Ag–ZnO Bent Cts nanocomposite	Ag	<0.005	<0.005
	Zn	<0.020	<0.020

for 30 min and 4 h of shaking (Table 3). The results revealed no leaching of either Ag or Zn into the water or the leaching amount was below the detection limits. The higher rate of Zn leaching can also be understood by referring to the EDS spectra [parts (a) and (c) of Fig. 4]. The EDS spectra indicate a high quantity of ZnO nanoparticles and a very low quantity of Ag nanoparticles within the Cts matrix, meaning that more ZnO is available to be exposed and released into the water. The present results were also compared with the ICP analysis of Bent nanocomposites (Ag Bent, ZnO Bent and Ag–ZnO nanocomposites) (Motshekga et al., 2013), and this comparison demonstrated that Bent Cts nanocomposites leached less. The stability of the nanoparticles in Bent Cts nanocomposites confirms that these materials are suitable for use in drinking water disinfection applications, as they comply with the standards set by WHO.

3.6. Evaluation of antibacterial activity

The antibacterial activities of cross-linked Cts and Bent Cts nanocomposites were tested against representative Gram-negative and Gram-positive bacteria, *E. coli* and *E. faecalis*, respectively. Parts

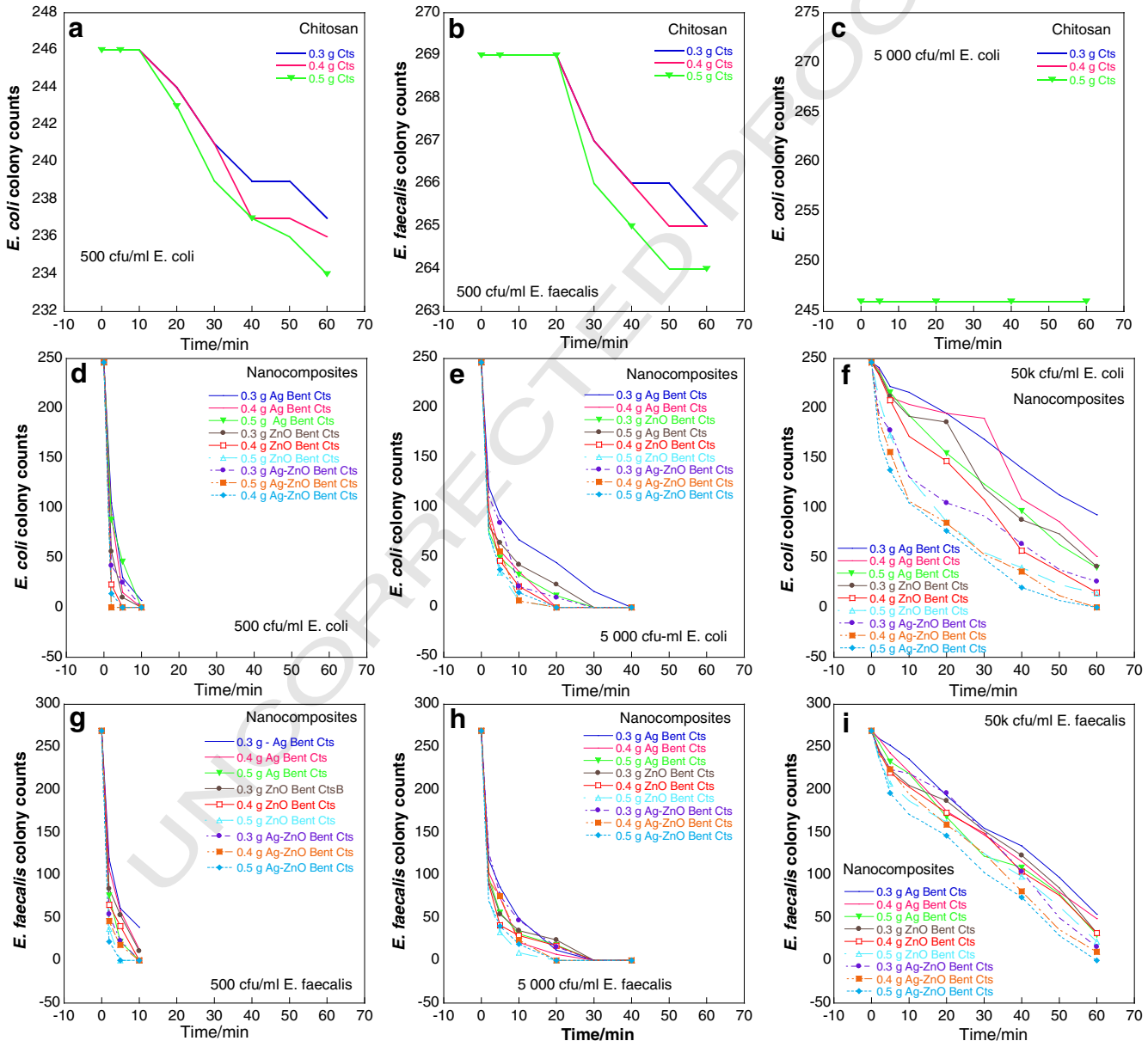

Fig. 5. Relations between contact time and colony counts of *E. coli* and *E. faecalis* at various bacterial concentrations: (a) three different weight percentages of Cts with 500 cfu/ml *E. coli*, (b) three different weight percentages of Cts with 500 cfu/ml *E. faecalis*, (c) three different weight percentages of Cts with 5000 cfu/ml *E. coli*, (d) three different weight percentages of various Bent Cts nanocomposites with 500 cfu/ml *E. coli*, (e) three different weight percentages of various Bent Cts nanocomposites with 5000 cfu/ml *E. coli*, (f) three different weight percentages of various Bent Cts nanocomposites with 50,000 cfu/ml *E. coli*, (g) three different weight percentages of various Bent Cts nanocomposites with 500 cfu/ml *E. faecalis*, (h) three different weight percentages of various Bent Cts nanocomposites with 5000 cfu/ml *E. faecalis*, (i) three different weight percentages of various Bent Cts nanocomposites with 50,000 cfu/ml *E. faecalis*.

Please cite this article as: Motshekga, S.C., et al., Preparation and antibacterial activity of chitosan-based nanocomposites containing bentonite-supported silver and zinc oxide nanoparticles for water disinfection, Appl. Clay Sci. (2015), http://dx.doi.org/10.1016/j.clay.2015.06.010

(a) to (i) of Fig. 5 present the relations between colony count and contact time for three different bacterial concentrations. Both *E. coli* and *E. faecalis* bacteria exhibited significant resistance to cross-linked Cts [parts (a) to (c) of Fig. 5]. As the bacterial concentration was increased, the time required to reduce the number of colonies increased. A slight reduction in colony count was illustrated after 40 min of contact time with 500 cfu/ml bacterial concentration. These observations can be understood in terms of the factors affecting the antibacterial efficiency of Cts, one of which is pH. It has been reported that at pH 7, at which the synthetic bacteria-contaminated water used in this study was prepared, Cts does not demonstrate any bactericidal activity because of the presence of a significant proportion of uncharged —NH_2 groups. Antibacterial activity of Cts has been reported at a pH below the corresponding pKa (pH 6.3), the value at which the soluble molecule disassociates into ions in solution. At a pH below the pKa, the positively charged —NH_2 group in Cts can interact with the negatively charged bacteria surface molecules which may result in the leakage of the intracellular constituents and hence causing cell death. At this pH, the —NH_2 groups are more active compared to a neutral pH (Kong et al., 2010; Regiel et al., 2013). However, pH is not the only factor that affects the antibacterial activity of Cts; the size of the particles and the specific surface area also play significant roles. Takahashi et al. (2008) have reported a similar study using Cts, in which they found that the antibacterial activity of Cts was influenced by the size of the powdered Cts, its shape and its specific surface area. In this study, the powdered Cts was sieved to <400 μm, and the surface area was 0.0695 m^2/g. Therefore, because the Cts used in this study possessed both a larger particle size and a lower surface area than the Cts investigated by Takahashi, it can be concluded that the same factors reported by Takahashi could have had significant effects on the antibacterial activity of Cts investigated here.

In contrast to the results obtained for Cts, Bent Cts nanocomposites demonstrated good antibacterial activity (parts (d) to (i) of Fig. 5). The antibacterial activity of Bent Cts nanocomposites against *E. coli* was found to be slightly higher than that against *E. faecalis* at all tested bacterial concentrations, as indicated by the colony counts. After a given contact time, there were consistently fewer viable colonies of *E. coli* than of *E. faecalis*. The counts decreased with increasing contact time and increased with increasing bacterial concentration. These findings can be explained in terms of the bacterial cell walls. *E. coli*, as a Gram-negative bacterium, is characterized by a thin cell wall, which means it is easier to penetrate than the thick cell wall of the Gram-positive bacterium *E. faecalis* (Kim et al., 2007). Similarly, the contact time played a critical role in the inactivation of bacteria. The time required to reduce the number of colonies increased with increasing bacterial concentration. For instance, the number of viable colonies was reduced to zero within 2 min (Fig. 5g) at the lowest bacterial concentration (500 cfu/ml), whereas at a high concentration of 5000 cfu/ml, 20 min was required (Fig. 5h). This also confirmed that more contact time was required when higher concentrations were employed. These observations are in agreement with the study of Gangadharan et al. (2010), in which the authors demonstrated that the inactivation of 10–300 × 10^6 cfu/ml of various bacteria was dependent on the contact time and the amount of polymer nanocomposite used. Their study demonstrated that after the first 2 h, there were still bacteria present in the treated water, whereas complete inactivation was achieved after 4 h, and the results differed between Gram-negative and Gram-positive bacteria.

A comparison on the performances of Ag Bent Cts nanocomposite and ZnO Bent Cts nanocomposite in reducing the number of bacterial colonies in the water indicated that ZnO Bent Cts nanocomposite was more effective than Ag Bent Cts nanocomposite. Both Bent Cts nanocomposites

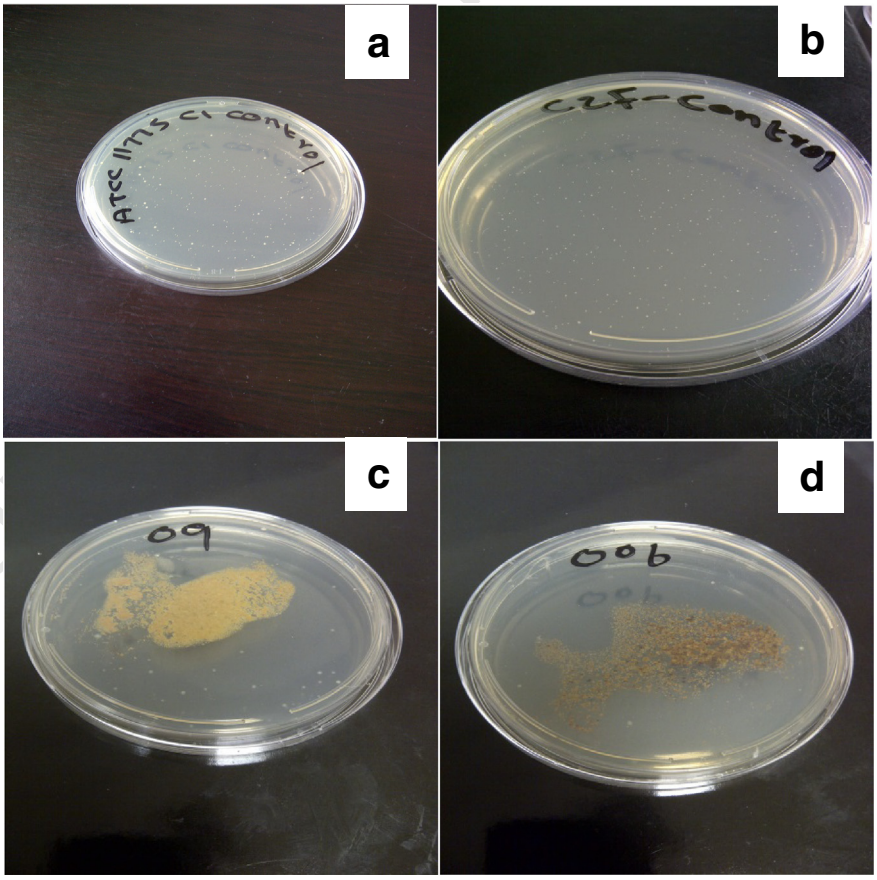

Fig. 6. Photographs of representative Petri dishes containing (a–b) control samples and (c–d) adsorbed/adhered bacteria-treated samples.

Please cite this article as: Motshekga, S.C., et al., Preparation and antibacterial activity of chitosan-based nanocomposites containing bentonite-supported silver and zinc oxide nanoparticles for water disinfection, Appl. Clay Sci. (2015), http://dx.doi.org/10.1016/j.clay.2015.06.010

achieved total inactivation of bacteria within the first 10 and 15 min for ZnO Bent Cts nanocomposite and Ag Bent Cts nanocomposite, respectively. In the case of Ag–ZnO Bent Cts nanocomposite, complete inactivation was illustrated within the first 2 min at bacterial concentrations of 500 cfu/ml for both bacteria, and more surviving colonies were identified as the bacterial concentration was increased. The more rapid bacterial inactivation demonstrated by ZnO Bent Cts nanocomposite and Ag–ZnO Bent Cts nanocomposite, may be explained in terms of the amount of nanoparticles present within Bent Cts nanocomposites. The EDS spectra indicated that Bent Cts nanocomposites contained more ZnO (21 wt.%) than Ag (3.9 wt.%), suggesting that ZnO should achieve more rapid inactivation. All three Bent Cts nanocomposites (Ag Bent Cts, ZnO Bent Cts and Ag–ZnO Cts nanocomposites) proved to exhibit antibacterial activity against both bacterial species, with a strong relation between the number of viable colonies and the contact time. The conclusions that can be drawn from these results are that the inactivation of bacteria is dependent on the contact time, and it is likely that all factors influencing the antibacterial activity of Cts also affected the antibacterial activity of Bent Cts nanocomposites but with different intensities. These results also demonstrate that a moderate inactivation effect is exerted by all Bent Cts nanocomposites independent of the bacterial cell walls and the amount of nanoparticles present, although at higher bacterial concentrations, more contact time is necessary for complete inactivation.

3.7. Testing for adsorption/adhesion of bacteria on cross-linked Cts and Bent Cts nanocomposites

After completion of the antibacterial experiments, the bacteria-contaminated water was decanted, and the residual material was poured onto an agar plate inoculated with bacteria and incubated for 24 h at 37 °C. This was done to test whether the material was acting as an adsorbent or a disinfectant or both. From the results obtained (Fig. 6), it was difficult to conclude whether the material was acting as an adsorbent or a disinfectant. The control samples [parts (a) and (b) of Fig. 6] showed bacterial growth, while few colonies accompanied by a small inhibition zone was measured near the decanted material [parts (c) and (d) of Fig. 6], which may indicate that the material behaved as both an adsorbent and a disinfectant.

4. Conclusions

Cts cross-linked with GLA and Bent Cts nanocomposites were successfully prepared using the solvent-casting method. Cts, a versatile material with proven antibacterial activity, did not demonstrate antibacterial activity against bacteria tested in this study. Previous studies revealed that factors such as pH, surface area and bacterial concentration play major roles in determining the antibacterial activity of Cts, which may have influenced the results obtained for Cts in this study. The nanoparticles in the Bent Cts nanocomposites were proven to be stable, with leaching below the accepted WHO standards. The antibacterial activity of Bent Cts nanocomposites was demonstrated to be dependent on the contact time, where the colony counts were revealed to decrease with increasing contact time in the presence of Bent Cts nanocomposites. Additionally, at higher bacterial concentrations, Bent Cts nanocomposites yielded better inactivation results for more contact time and a greater amount of Bent Cts nanocomposites. From these results, it is apparent that cross-linked Cts alone is ineffective in achieving the complete inactivation of the studied bacteria, and hence, it is imperative to synthesize Bent Cts nanocomposites. The results also indicate that the investigated Bent Cts nanocomposites are potential antibacterial materials that may be used to combat waterborne bacteria.

Acknowledgments

The authors (SCM and SSR) wish to thank DST and CSIR, South Africa, for their financial support. Q10 Q11

References

Anirudhan, T.S., Rijith, S., 2009. Glutaraldehyde cross-linked epoxyaminated chitosan as an adsorbent for the removal and recovery of copper (II) from aqueous media. Colloids Surf. A Physicochem. Eng. Asp. 351, 52–59.

Ayari, F., Srasra, E., Trabelsi-Ayadi, M., 2005. Characterization of bentonitic clays and their use as adsorbent. Desalination 185, 391–397.

Azam, A., Ahmed, A.S., Oves, M., Khan, M.S., Habib, S.S., Memic, A., 2012. Antimicrobial activity of metal oxide nanoparticles against Gram-positive and Gram-negative bacteria: a comparative study. Int. J. Nanomedicine 7, 6003–6009.

Bagchi, B., Kar, S., Dey, S.K., Bhandary, S., Roy, D., Mukhopadhyay, T.K., Das, S., Nandy, P., 2013. In situ synthesis and antibacterial activity of copper nanoparticle loaded natural montmorillonite clay based on contact inhibition and ion release. Colloids Surf. B: Biointerfaces 108, 358–365.

Beppu, M.M., Vieira, R.S., Aimoli, C.G., Santana, C.C., 2007. Crosslinking of chitosan membranes using glutaraldehyde: effect on ion permeability and water absorption. J. Membr. Sci. 301, 126–130.

Bhattacharyya, K.G., Gupta, S.S., 2006. Pb(II) uptake by kaolinite and montmorillonite in aqueous medium: influence of acid activation of the clays. Colloids Surf. A Physicochem. Eng. Asp. 277, 191–200.

Boorman, G.A., Dellarco, V., Dunnick, J.K., Chapin, R.E., Hunter, S., Hauchman, F., Gardner, H., Cox, M., Sills, R.C., 1999. Drinking water disinfection byproducts: review and approach to toxicity evaluation. Environ. Health Perspect. 107 (1), 207–217.

Chang, M.Y., Juang, R.S., 2004. Adsorption of tannic acid, humic acid, and dyes from water using the composite if chitosan and activated clay. J. Colloid Interface Sci. 278, 18–25.

dos Santos, C.A., Jozala, A.F., Pessoa Jr., A., Seckler, M.M., 2012. Antimicrobial effectiveness of silver nanoparticles co-stabilized by the bioactive copolymer pluronic F68. J. Nanobiotechnol. 10, 1–6.

El-Sherif, H., El-Masry, M., 2011. Superabsorbent nanocomposite hydrogels based on intercalation of chitosan into activated bentonite. Polym. Bull. 66 (6), 721–734.

Emami-Karvani, Z., Chehrazi, P., 2011. Antibacterial activity of ZnO nanoparticle on Gram-positive and Gram-negative bacteria. Afr. J. Microbiol. Res. 5, 1368–1373.

Gangadharan, D., Harshvardan, K., Gnanasekar, G., Dixit, D., Popat, K.M., Anand, P.S., 2010. Polymeric microspheres containing silver nanoparticles as a bactericidal agent for water disinfection. Water Res. 44, 5481–5487.

Guibal, E., Cambe, S., Bayle, S., Taulemesse, J.M., Vincent, T., 2013. Silver/chitosan/cellulose fibers foam composites: from synthesis to antibacterial properties. J. Colloid Interface Sci. 393, 411–420.

Hashemian, S., 2010. $MnFe_2O_4$/bentonite nano composite as a novel magnetic material for adsorption of acid red 138. Afr. J. Biotechnol. 9 (50), 8667–8671.

Hrenovic, J., Milenkovic, J., Ivankovic, T., Rajic, N., 2012. Antibacterial activity of heavy metal-loaded natural zeolite. J. Hazard. Mater. 201–202, 260–264.

Jones, N., Ray, B., Ranjit, K.T., Manna, A.C., 2008. Antibacterial activity of ZnO nanoparticle suspensions on a broad spectrum of microorganisms. FEMS Microbiol. Lett. 279, 71–76.

Kamari, A., Wan Ngah, W.S., Chong, M.Y., Cheah, M.L., 2009. Sorption of acid dyes onto GLA and H_2SO_4 cross-linked chitosan beads. Desalination 249, 1180–1189.

Karapinar, N., Donat, R., 2009. Adsorption behaviour of Cu^{2+} and Cd^{2+} onto natural bentonite. Desalination 249, 123–129.

Kim, J.S., Kuk, E., Yu, K.N., Kim, J.H., Park, S.J., Lee, H.J., Kim, S.H., Park, Y.K., Park, Y.H., Hwang, C.Y., Kim, Y.K., Lee, Y.S., Jeong, D.H., Cho, M.H., 2007. Antimicrobial effects of silver nanoparticles. Nanomedicine 3, 95–101.

Kittinaovarat, S., Kansomwan, P., Jiratumnukul, N., 2010. Chitosan/modified montmorillonite beads and adsorption Reactive Red 120. Appl. Clay Sci. 48, 87–91.

Kong, M., Chen, X.G., Xing, K., Park, H.J., 2010. Antimicrobial properties of chitosan and mode of action: a state of the art review. Int. J. Food Microbiol. 144 (1), 51–63.

Krasner, S.W., Weinberg, H.S., Richardson, S.D., Pastor, S.J., Chinn, R., Sclimenti, M.J., Onstad, G.D., Thruston Jr., A.D., 2006. Occurrence of a new generation of disinfection byproducts. Environ. Sci. Technol. 40, 7175–7185.

Li, Q.L., Mahendra, S., Lyon, D.Y., Brunet, L., Liga, M.V., Li, D., Alvarez, P.J.J., 2008. Antimicrobial nanomaterials for water disinfection and microbial control: potential applications and implications. Water Res. 42, 4591–4602.

Li, L.H., Deng, J.C., Deng, H.R., Liu, Z.L., Li, X.L., 2010. Preparation, characterization and antimicrobial activities of chitosan/Ag/ZnO blend films. Chem. Eng. J. 160 (1), 378–382.

Li, B., Shan, C.L., Zhou, Q., Fang, Y., Wang, Y.L., Xu, F., Han, L.R., Ibrahim, M., Guo, L.B., Xie, G.L., Sun, G.C., 2013. Synthesis, characterization, and antibacterial activity of cross-linked chitosan-glutaraldehyde. Mar. Drugs 11, 1534–1552.

Lin, S., Huang, R., Cheng, Y., Liu, J., Lau, B.L.T., Wiesner, M.R., 2012. Silver nanoparticle–alginate composite beads for point-of-use drinking water disinfection. Water Res. 47, 3959–3965.

Magaña, S.M., Quintana, P., Aguilar, D.H., Toledo, J.A., Ángeles-Chávez, C., Cortés, M.A., León, L., Freile-Pelegrín, Y., López, T., Torres Sánchez, R.M., 2008. Antibacterial activity of montmorillonites modified with silver. J. Mol. Catal. A Chem. 281 (1–2), 192–199.

Meteš, A., Kovačević, D., Vujević, D., Papić, S., 2004. The role of zeolites in wastewater treatment of printing inks. Water Res. 38 (14–15), 3373–3381.

Motshekga, S.C., Ray, S.S., Onyango, M.S., Momba, M.N., 2013. Microwave-assisted synthesis, characterization and antibacterial activity of Ag/ZnO nanoparticles supported bentonite clay. J. Hazard. Mater. 262, 439–446.

Please cite this article as: Motshekga, S.C., et al., Preparation and antibacterial activity of chitosan-based nanocomposites containing bentonite-supported silver and zinc oxide nanoparticles for water disinfection, Appl. Clay Sci. (2015), http://dx.doi.org/10.1016/j.clay.2015.06.010

Özcan, A.S., Özcan, A., 2004. Adsorption of acid dyes from aqueous solutions onto acid-activated bentonite. J. Colloid Interface Sci. 276 (1), 39–46.
Prüss-Üstün, A., Bos, R., Gore, F., Bartram, J., 2008. Safer Water, Better Health: Costs, Benefits and Sustainability of Interventions to Protect and Promote Health. WHO, Geneva.
Quang, D.V., Chau, N.H., 2013. The effect of hydrothermal treatment on silver nanoparticles stabilized by chitosan and its possible application to produce mesoporous silver powder. J. Powder Technol. 13, 1–6.
Raafat, D., Sahl, H.G., 2009. Chitosan and its antimicrobial potential — a critical literature survey. Microb. Biotechnol. 2, 186–201.
Raghupathi, K.R., Koodali, R.T., Manna, A.C., 2011. Size-dependent bacterial growth inhibition and mechanism of antibacterial activity of zinc oxide nanoparticles. Langmuir 27, 4020–4028.
Ray, P.C., Khan, S.A., Singh, A.K., Senapati, D., Fan, Z., 2012. Nanomaterials for targeted detection and photothermal killing of bacteria. Chem. Soc. Rev. 41 (8), 3193–3209.
Reddy, K.M., Feris, K., Bell, J., Wingett, D.G., Hanley, C., Punnoose, A., 2007. Selective toxicity of zinc oxide nanoparticles to prokaryotic and eukaryotic systems. Appl. Phys. Lett. 90 (213902), 2139021–2139023.
Regiel, A., Irusta, S., Kyzioł, A., Arruebo, M., Santamaria, J., 2013. Preparation and characterization of chitosan–silver nanocomposite films and their antibacterial activity against *Staphylococcus aureus*. Nanotechnology 24, 1–13.
Richardson, S.D., 2003a. Disinfection by-products and other emerging contaminants in drinking water. Trends Anal. Chem. 22, 666–684.
Richardson, S.D., 2003b. Water analysis: emerging contaminants and current issues. Anal. Chem. 75, 2831–2857.
Richardson, S.D., 2004. Environmental mass spectrometry: emerging contaminants and current issues. Anal. Chem. 76 (12), 3337–3364.
Santos, M.F., Oliveira, C.M., Tachinski, C.T., Fernandes, M.P., Pich, C.T., Angioletto, E., Riella, H.G., Fiori, M.A., 2011. Bactericidal properties of bentonite treated with Ag^{+} and acid. Int. J. Miner. Process. 100, 51–53.
Savage, N., Diallo, M.S., 2005. Nanomaterials and water purification: opportunities and challenges. J. Nanoparticle Res. 7, 331–342.
Shahverdi, A.R., Fakhimi, A., Shahverdi, H.R., Minaian, M.S., 2007. Synthesis and effect of silver nanoparticles on the antibacterial activity of different antibiotics against *Staphylococcus aureus* and *Escherichia coli*. Nanomedicine 3, 168–171.
Shameli, K., Ahmad, M.B., Zin, W.M., Yunus, W., Rustaiyan, A., Ibrahim, N.A., Zargar, M., Abdollahi, Y., 2010. Green synthesis of silver/montmorillonite/chitosan bionanocomposites using the UV irradiation method and evaluation of antibacterial activity. Int. J. Nanomedicine 5, 875–887.
Shameli, K., Ahmad, M.B., Zargar, M., Yunus, W.M., Rustaiyan, A., Ibrahim, N.A., 2011a. Synthesis of silver nanoparticles in montmorillonite and their antibacterial behaviour. Int. J. Nanomedicine 6, 581–590.
Shameli, K., Ahmad, M.B., Zargar, M., Yunus, W.M., Ibrahim, N.A., Shabanzadeh, P., Moghaddam, M.G., 2011b. Synthesis and characterization of silver/montmorillonite/chitosan bionanocomposites by chemical reduction method and their antibacterial activity. Int. J. Nanomedicine 6, 271–284.
Standard Methods for examination of water and wastewater, 20th ed., AWWA, Water Environment Federation, APHA, Washington, DC, USA, 1998.
Takahashi, T., Imai, M., Suzuki, I., Sawai, J., 2008. Growth inhibitory effect of bacteria on chitosan membranes regulated by the deacetylation degree. Biochem. Eng. J. 40, 485–491.
Talebian, N., Amininezhad, S.M., Doudi, M., 2013. Controllable synthesis of ZnO nanoparticles and their morphology-dependent antibacterial and optical properties. J. Photochem. Photobiol. B Biol. 120, 66–73.
Theivasanthi, T., Alagar, M., 2011. Antibacterial studies of silver nanoparticles. Gen. Phys. (arXiv:1101.0348 [physics.gen-ph]. Accessed 23 April 2013). Q12
Tiwari, D.K., Behari, J., Sen, P., 2008. Application of nanoparticles in waste water treatment. World Appl. Sci. J. 3, 417–433.
Wang, S.F., Shen, L., Tong, Y.J., Chen, L., Phang, I.Y., Lim, P.Q., Liu, T.X., 2005. Biopolymer chitosan/montmorillonite nanocomposites: preparation and characterization. Polym. Degrad. Stab. 90, 123–131.
WHO World Water Day Reporthttp://www.who.int/water_sanitation_health/takingcharge (Accessed December 2013).
Woo, Y.T., Lai, D., McLain, J.L., Manibusan, M.K., Dellarco, V., 2002. Use of mechanism-based structure–activity relationships analysis in carcinogenic potential ranking for drinking water disinfection by-products. Environ. Health Perspect. 110, 75–88.
World Health Organization, 2006a. Emerging Issues in Water and Infectious Disease. WHO, Geneva.
World Health Organization, 2006b. Guidelines for Drinking-water Quality. 3rd ed. vol. 1. WHO, Geneva.
World Health Organization, 2011. Guidelines for Drinking-water Quality. 4th ed. vol. 1. WHO, Geneva.
Yavuza, Ö., Altunkaynak, Y., Güzel, F., 2003. Removal of copper, nickel, cobalt and manganese from aqueous solution by kaolinite. Water Res. 37, 948–952.
Zamparas, M., Gianni, A., Stathi, P., Deligiannakis, Y., Zacharias, I., 2012. Removal of phosphate from natural waters using innovative modified bentonites. Appl. Clay Sci. 62–63 (1), 101–106.
Zheng, L.Y., Zhu, J.F., 2003. Study on antimicrobial activity of chitosan with different molecular weights. Carbohydr. Polym. 54, 527–530.

Please cite this article as: Motshekga, S.C., et al., Preparation and antibacterial activity of chitosan-based nanocomposites containing bentonite-supported silver and zinc oxide nanoparticles for water disinfection, Appl. Clay Sci. (2015), http://dx.doi.org/10.1016/j.clay.2015.06.010